Available online at www.sciencedirect.com

SCIENCE DIRECT®

Vision Research 44 (2004) 2445–2456

Vision Research

www.elsevier.com/locate/visres

In vivo biometry in the mouse eye with low coherence interferometry

Christine Schmucker, Frank Schaeffel *

Section of Neurobiology of the Eye, University Eye Hospital, Calwerstr. 7/1, 72076 Tuebingen, Germany

Received 25 March 2004; received in revised form 17 May 2004

Abstract

Purpose. A major drawback of the mouse model of myopia is that the ocular dimensions cannot be measured in vivo, and that histological techniques post-mortem suffer from limited resolution. We have tested the potential of a newly developed technique, optical low coherence interferometry (OLCI), adapted for short measurement distances by Meditec, Carl Zeiss, Jena, Germany (the "ACMaster"). Using this technique, ocular biometry was performed in mice with normal vision and after deprivation of form vision.

Methods. Axial eye length, corneal thickness and anterior chamber depth were measured in 23 mice, aged 25–53 days, and standard deviations from repeated measurements in the same eyes, as well as intra-individual and inter-individual variability were determined in different age groups. The data were compared to those from a preceding study in which biometrical data were obtained from frozen sections [Vision Res. 44 (2004) 1857]. Refractions were measured by automated infrared photorefraction. Mice had either normal visual exposure or were monocularly deprived of form vision for 14 days.

Results. Using OLCI, axial length could be determined with an average standard deviation of 8.0 ± 2.9 μm, corneal thickness with 3.5 ± 2.1 μm, and anterior chamber depth with 10.6 ± 12.3 μm. Neither axial length, nor corneal thickness, nor anterior chamber depth were significantly different in left and right eyes of individual mice that had normal visual experience (mean absolute difference between axial lengths: 17 ± 18 μm, between corneal thickness 5.1 ± 4.8 μm, and between anterior chamber depths 16.7 ± 14.8 μm). Compared to the variability that was previously found in frozen sections, the variability of axial length measurements with OLCI was 2.7 times less. After two weeks of form deprivation, OLCI revealed a significant axial elongation in the occluded eyes, compared to the contralateral fellow eyes (+38 ± 36 μm or 1.16%, $p = 0.045$, $n = 7$, paired t-test). In this sample, no accompanying myopic shift was observed in the occluded eyes but this observation is not unexpected given the inherently variable responses of mouse eye growth to visual deprivation.

Conclusion. OLCI had sufficient resolution in living mice to detect axial length changes in vivo that were equivalent to a dioptric change of 2 D. Using this technique, it was confirmed that mouse eyes respond to form deprivation by axial elongation, similar to the eyes of other animal models. The lack of a myopic shift in this sample, despite the axial elongation, demonstrates that biometric data are particularly important when the mouse eye is used as a model to study myopia.

1. Introduction

Animal models have greatly extended our understanding of the aetiology of myopia (i.e. Hung, Crawford, & Smith, 1995; Rada, Nickla, & Troilo, 2000; Schaeffel, Bartmann, Hagel, & Zrenner, 1995; Troilo, Nickla, & Wildsoet, 2000). Deprivation of form vision during a critical period of development has been shown to induce myopia in a wide range of species for example in monkeys, tree shrews, chickens, squirrels, guinea pigs and, as described most recently, in mice. It has been emphasized before that the mouse is a promising model to study genetic influences in myopia (Schaeffel, Simon,

* Corresponding author. Tel.: +49-7071-2980739; fax: +49-7071-295196.

E-mail address: frank.schaeffel@uni-tuebingen.de (F. Schaeffel).

URL: http://www.uak.medizin.uni-tuebingen.de/frank.

0042-6989/$ - see front matter © 2004 Elsevier Ltd. All rights reserved.
doi:10.1016/j.visres.2004.05.018

Feldkaemper, Ohngemach, & Williams, 2003; Schaeffel, Burkhardt, Howland, & Williams, 2004; Zhou & Williams, 1999).

Unfortunately, due to the lack of appropriate techniques to measure ocular dimensions in mice in vivo, axial length data are either missing (Schaeffel & Burkhardt, 2002) or have undetermined reliability (histological technique: Tejedor & de la Villa, 2003; Schaeffel & Howland, 2003; digital calliper: Beuerman, Barathi, Weon, & Tan, 2003). The standard technique for in vivo biometry in vertebrate eyes is A-scan ultrasonography. However, due to the steep curvature of the mouse cornea, the contact area of the ultrasound transducer is too small to transmit sufficient sound energy into the eye for a satisfactory signal to noise ratio. Furthermore, most ultrasound transducers focus their energy at a certain distance which is adapted to the length of the human eye. Obviously, the axial length of the mouse eye is too short to obtain interpretable echoes. Finally, the spatial resolution of ultrasound devices is limited by their wavelength and, typically, does not exceed 40 μm, equivalent to almost 10 D in a mouse eye (Schmucker & Schaeffel, 2004).

It is clear that alternative techniques are necessary. Recently, a novel non-contact pachymetric technique was described which is based on optical low coherence reflectometry. In a previous study, it was used to measure corneal thickness in mouse eyes in vivo (Schulz, Iliev, Frueh, & Goldblum, 2003). In the present study, we applied optical low coherence biometry to measure also axial length of the eyes of the C57BL/6 mouse eye in vivo. The optical low coherence interferometer (''OLCI''—implemented in the Carl Zeiss ''ACMaster'', Jena, Germany) was originally developed for measurements of the anterior depth and of lens thickness in living human eyes. Its spatial resolution was claimed to be in the range of 5–10 μm.

In the present study, its resolution was examined in tiny eyes of the mouse (about 3 mm axial length). The OLCI data were compared with biometric data which were previously obtained in measurements in frozen sections (Schmucker & Schaeffel, 2004). Furthermore, it was attempted to verify that visual deprivation causes indeed axial elongation in mice, similar to in other animal models of myopia.

2. Material and methods

2.1. Animals

All experiments were conducted in accordance with the ARVO Statement for the Use of Animals in Ophthalmic and Vision Research. The treatment of the mice was approved by the University commission for animal welfare (reference AK3/02). Black C57BL/6 wildtype mice were obtained from Charles River GmbH, Sulzfeld, Germany, and bred in the animal facilities of the Institute. Untreated animals were housed in groups of 6–8 while animals wearing occluders were housed individually in standard mouse cages under a 12 h light/dark cycle. Ambient illuminance was provided by incandescent lights and was about 500 lux on the cage floor (measured with a calibrated photo cell [United Detector Technology] in photometric mode).

2.2. Measurement principle

Biometrical data of the mouse eye were collected with a new device based on OLCI, the Carl Zeiss ''ACMaster'' (http://www.meditec.zeiss.com/). The principle of OLCI is based on a Michelson interferometer (Fig. 1). The light source is a low coherence superluminescent laser diode (SLD) that emits an infrared light with a peak emission at 850 nm and a half-band width of 10 nm. Due to the broadened bandwidth, the coherence length is rather short (about 10 μm), compared to standard laser diodes, in which it is about 160 μm. Output energy is 450 μW. The infrared laser beam emerging from the LED is divided into two perpendicular beams by a semi-silvered mirror. One part is transmitted through the semi-silvered mirror and reaches a stationary mirror. The other part is reflected and reaches a mirror that can be moved along the light path with high positional precision. After reflection from both mirrors, two coaxial beams of about 50 μm diameter propagate to the eye, where they are reflected off from the cornea, the lens and the retinal pigment epithelium (RPE) close to the vitreo-retinal interface. Interference between both beams can only occur when their optical path lengths are matched within the coherence length. The occurrence of interference is detected by a photo cell and recorded as a function of the displacement of the movable mirror. Due to the usage of coaxial beams, the measurements are largely insensitive against longitudinal eye movements. The scanning time of the movable mirror is about 0.3 s. The resolution of the system is limited both by the coherence length, which is inversely proportional to the bandwidth of the SLD, and by the precision by which the position of the movable mirror can be controlled. In the human eye, a measurement precision in the range of 2 μm has been described in corneal thickness measurements and of 5–10 μm for the anterior chamber depth and lens thickness measurements (R. Bergner, Carl Zeiss, Jena, personal communication 2004).

The major reflections in the eye occur at the anterior corneal surface and at the RPE. Accordingly, the interference signals are most conspicuous at these two layers.

The software of the ''ACMaster'' is designed to measure the anterior segment in human eyes. This means that it expects to find reflecting surfaces at

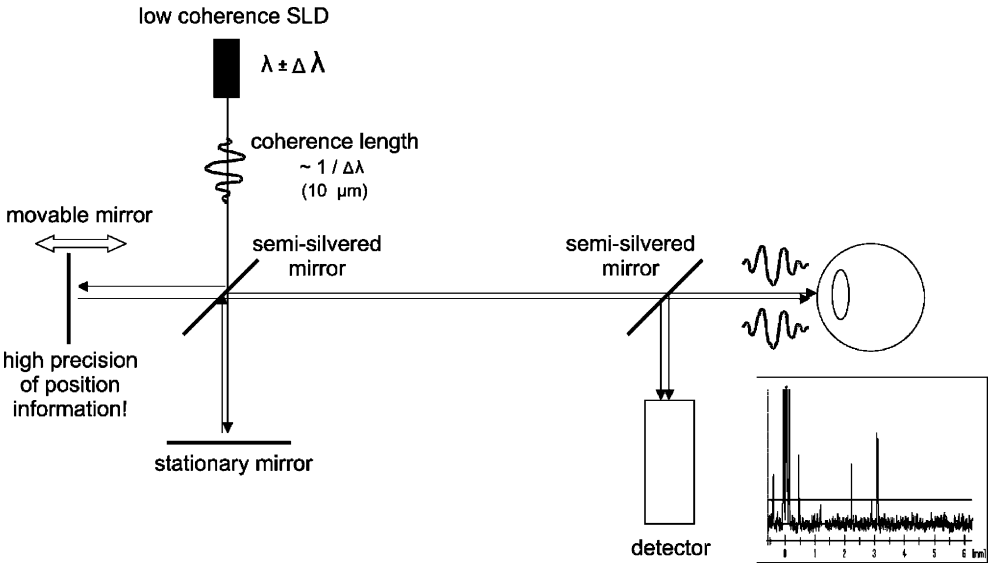

Fig. 1. Schematic illustration of the low coherence interferometer implemented in the Zeiss "ACMaster". SLD: superluminescent diode. The beam emitted from the SLD is either transmitted through the semi-silvered mirror and reflected from a stationary mirror, or reflected at the semi-silvered mirror and then reflected from the movable mirror. Both reflected beams propagate to the eye. If their path length is matched within the coherence length, they display interference. The interference pattern is detected by a detector and displayed on the monitor of the device. The movable mirror is shifted along the measurement axis with very high precision. Once interference is achieved, the corresponding position of the movable mirror provides the information on the position of the respective reflecting surface in the eye.

about 0.5 mm behind the anterior corneal surface (which would correspond to the thickness of the human cornea) and a second major reflection between 2 and 5 mm distance (the anterior surface of the lens). The software could be used to measure mouse eyes because reflecting surfaces were present within the ranges accepted by the software: the distance to the anterior surface of the lens of the mouse eye is in the range of the thickness of the human cornea, and the distance to the RPE in the back of the eye is in the range of the distance of the anterior lens surface in human eyes. This means that the software had to detect anterior corneal surface, anterior lens surface, and the RPE to provide biometric data (Fig. 2). Anterior chamber depth, as plotted below, is defined as the distance from the anterior corneal surface to the anterior surface of the lens. The peak of the posterior lens surface was detected only in a few measurements. Therefore no consistent data on lens thickness are provided.

To measure corneal thickness in the mouse eye, the cursor that was automatically placed at the anterior lens surface was manually moved anteriorly, to the back of the cornea. The lens surface position was no longer measured in this case. However, the measured axial length was then longer because the length of the path of the

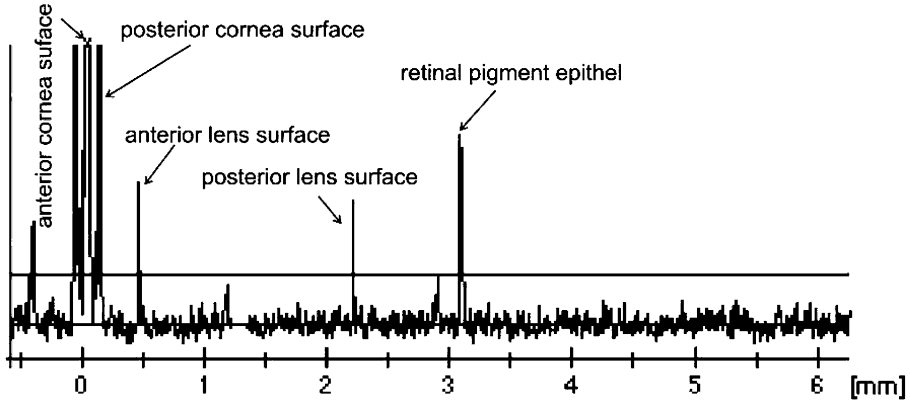

Fig. 2. Low coherence interferogram of the mouse eye. The intensity of the peaks is plotted versus the optical path length. The origin of the reflections of the cornea layers, the lens and the RPE are shown. The peak of the posterior lens surface was detected only in a few of the measurements. Therefore, a consistent evaluation of lens thickness was not possible.

light through the optical medium with higher refractive index was shorter (see experimental confirmation below).

The device used a refractive index of 1.3851 for the human cornea and an index of 1.3454 for the aqueous humor. That means that the measurements in the mouse eye are based on an index of 1.3851 for the anterior chamber and/or corneal thickness and an average index of 1.3454 for lens and vitreous humor, which both may not be the best approximation. Accordingly, it is expected that the device overestimates axial length (experimental confirmation see below).

2.3. In vivo measurement procedure

All measurements were performed between 10 a.m. and 4 p.m. Prior to the measurements, mice were anaesthetized with an subcutane injection of 0.1–0.2 ml of a mixture of 1.2 ml 10% ketamine hydrochloride and 0.8 ml 2% xylazine hydrochloride, dissolved in 8.0 ml sterile saline. Subsequently, the animals were positioned on a adjustable platform that was screwed to the chinrest of the device (Fig. 3A). The pupil axis of the eye was aligned with the measurement axis, and the distance of the eye to the measurement head was adjusted to approximately 70 mm, using six infrared LEDs arranged in a circle that were imaged on the cornea and focused under high magnification (Fig. 3B). Then, a series of approximately 20 longitudinal scans was performed within a few seconds. All animals recovered from the anesthesia and the measurements without complications.

After completing the measurements, the interferogram was analysed. In some scans, the relevant interfaces were not detected or were ambiguous. Only those scans which showed clear peaks at the cornea, the anterior lens surface and the retino-vitreal interface were used to calculate means and standard deviations (SD) of optical eye length, optical corneal thickness and optical anterior chamber depth in each eye.

2.4. Analysis of the measurements in untreated animals

Axial eye length, central corneal thickness and anterior chamber depth were measured in 23 mice with normal visual experience, at the ages of 25, 29, 35, 47 and 53 days. At least three mice were measured in each age group and the means and standard deviations were calculated separately for both eyes in each animal. The data for different age groups were compared to biometric data from a previous study in which the ocular dimensions were determined in frozen sections (Schmucker & Schaeffel, 2004).

To evaluate the differences between the left and the right eyes, mean values of axial length and their standard deviations from 19 untreated mice at different ages were plotted against each other and the absolute average differences between both eyes was calculated.

To analyze potential confounding effects of changes in orientation of the eyes during the measurements, the eyes in ten mice were voluntarily rotated in either the horizontal or vertical meridian. In these measurements, the Purkinje image of one of the six LEDs was positioned close to the pupil margin, 0.60 ± 0.06 mm away from its position when the circle (Fig. 3B) was centered in the pupil. With a Hirschberg ratio (= eye rotation necessary to displace the first Purkinje image by 1 mm) of 86.7 ± 3 (Schaeffel et al., 2004), the corresponding angles were $52 \pm 6°$ nasally, temporally, superiorly and inferiorly of the pupil axis.

2.5. Ocular development in form-deprived animals

One eye in seven mice was occluded by attaching handmade frosted hemispherical thin plastic shells to the fur around the eye as previously described (Schaeffel et al., 2004). In brief, the little shells of 8 mm diameter had a rim, about 1mm wide, that was glued to the fur around the eyes by instant glue (cyanyl acrylate) under light ether anesthesia on post natal day 27. Subsequently, thin plastic collars were fitted around the neck

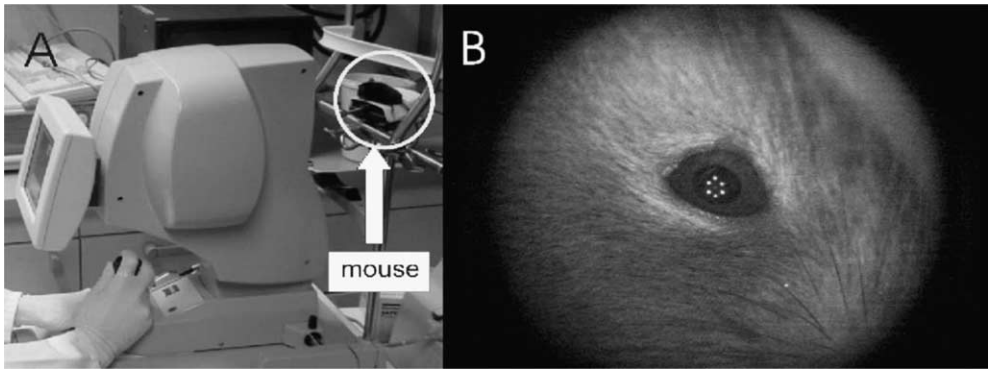

Fig. 3. (A) The "ACMaster" during measurements of a mouse eye. The anesthetized mouse, positioned on an adjustable platform which was attached to the chinrest of the device, is encircled. (B) Close-up view used to adjust the eye in the measurement beam. The first Purkinje images of six infrared LEDs, built into the device, were used to align the eye.

to prevent mice from removing their diffusers. The diffusers were removed on day 41. Refractive state, measured by infrared photoretinoscopy (Schaeffel et al., 2004), and ocular biometry by OLCI, were performed in anaesthetized animals both before and after the occlusion period.

The number of animals that were covered with diffusers were comparably small; however, previous occlusion experiments in 50 mice had shown that deprivation produces a highly significant change in refractive state in the myopic direction (see Section 4).

2.6. Statistical analysis

The performance of OLCI was studied in the different age groups by analyzing the standard deviations from repeated measurements in the same eyes. To study the effects of eye orientation on the measured axial lengths, a variance ratio test was used. The absolute differences between both eyes in individual animals were analyzed by paired *t*-tests to estimate the natural variability in eye length. Paired *t*-tests were used to compare occluded and open control eyes.

3. Results

3.1. Ocular dimensions in untreated animals

Mean values and standard deviations of axial length data are shown in Fig. 4. Axial length appeared slightly larger when it was determined after the cursor was manually moved from the anterior lens surface to the back surface of the cornea than when the anterior lens surface was automatically chosen by the software. However, this was expected, given the choices of the refractive indices (see Section 2).

Axial length displayed a slight regression in our sample at the age of 53 days (Fig. 4). Previous data, showing that the mouse eye grows continuously at least beyond the age of 100 days (Schmucker & Schaeffel, 2004), exclude that growth is already levelling off at this age. The cessation must rather be due to the fact that mice from different litters were used at each age level. Due to the satisfactory agreement between both methods, only data that were obtained with the cursor moved to the back of the cornea are shown below. A linear regression of axial eye length versus age shows that the eyes grow by 7.3 μm per day ($y=0.0073+2.9614$, $R^2=0.8613$).

3.1.1. Variability of axial length measurements and comparisons to data from frozen sections

The average standard deviation for axial length measurements, i.e. average of all standard deviations obtained in repeated measurements in individual eyes was 8.0 ± 2.9 μm. There were no significant differences among different age groups in this study (variance ratio test; $p>0.05$).

To determine how well the OLCI data were in agreement with the data from frozen sections, both data sets are plotted against age in Fig. 5. The growth rates determined with OLCI were significantly higher (slope of axial length versus age: OLCI: 0.00728 ± 0.00076, frozen section: 0.00511 ± 0.00051, df = 10, $T=5.5$, $p<0.001$; regression equations OLCI: $y=0.007x+2.961$, $R^2=0.861$; frozen section technique: $y=0.005x+2.873$, $R^2=0.745$). There was also a consistent overestimation of axial

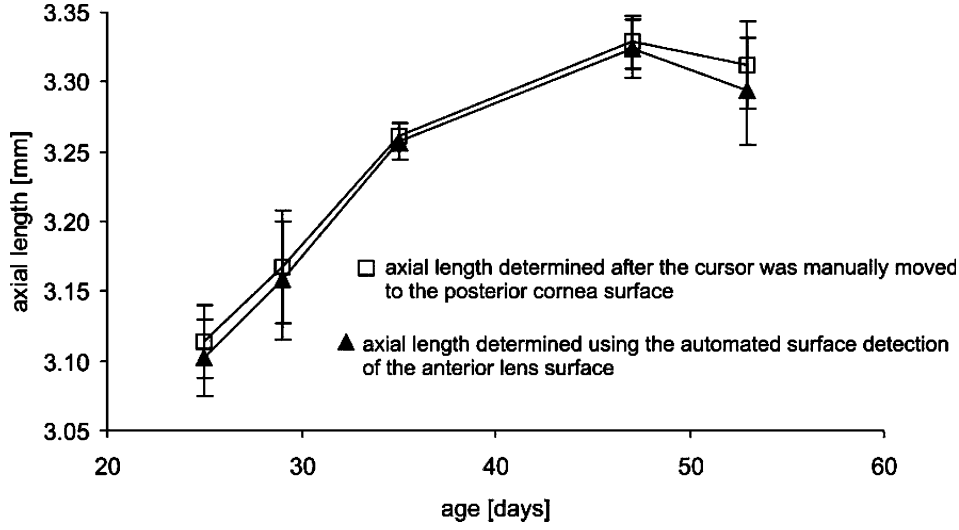

Fig. 4. Axial eye growth between day 25 and 53, as measured by OLCI. Axial length was determined either after the cursor was manually moved to the back of the cornea (upper curve) or by using the automated surface detection in the software of the "ACMaster" (lower curve). Data from 23 animals contributed to the curve, with $n=3$ or more animals for each data point. Error bars denote standard deviations.

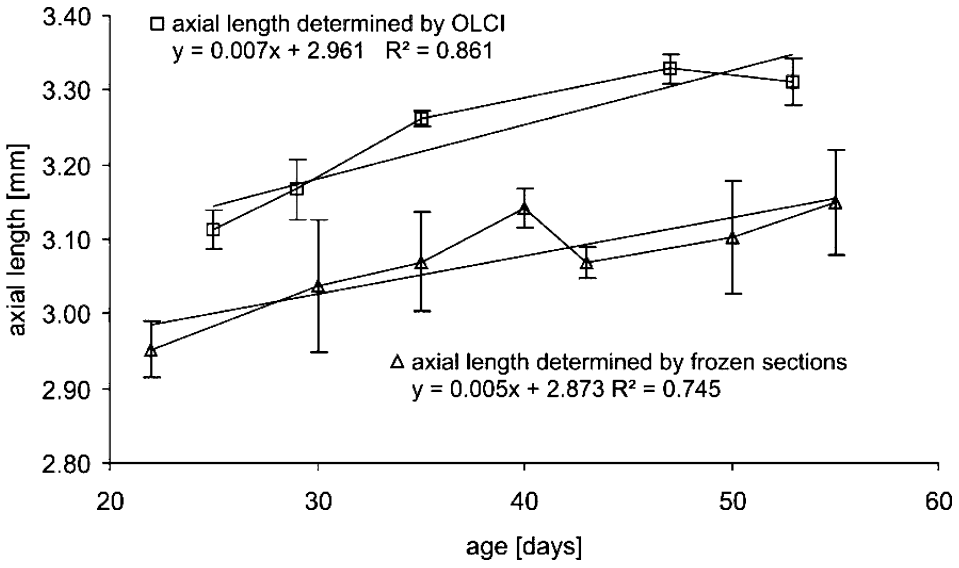

Fig. 5. Comparison of axial length measurements by OLCI and by frozen sections (frozen section data replotted after Schmucker and Schaeffel, 2004). Axial length determined by OLCI has a lower average standard deviation by a factor of 2.7. Error bars denote standard deviations.

lengths by OLCI by, on average, about 200 μm or 6.5%. Both differences trace back to inappropriate assumptions regarding the refractive indices to convert optical path length into geometrical path length. With an average refractive index of 1.433 (1.345 increased by 6.5%) for aqueous humor, lens and vitreous humor, both measurements produce very similar axial length.

The average standard deviations were smaller with OLCI by a factor of 2.7 (average standard deviation of the different age groups: 25 μm in OLCI, versus 68 μm in frozen sections).

3.1.2. Within-animal variability

To evaluate the resolution of OLCI in detecting differences between both eyes of a mouse, the axial lengths from the left and right eye are plotted against each other (Fig. 6). Orthogonal rather than linear regression was applied to study correlations between the eyes, since both data sets represent independent variables, with expected similar variance. First, there was no significant inter-ocular difference in any of the animals at any age group (paired t-tests, $p > 0.095$). Second, the average absolute differences in axial lengths between both eyes

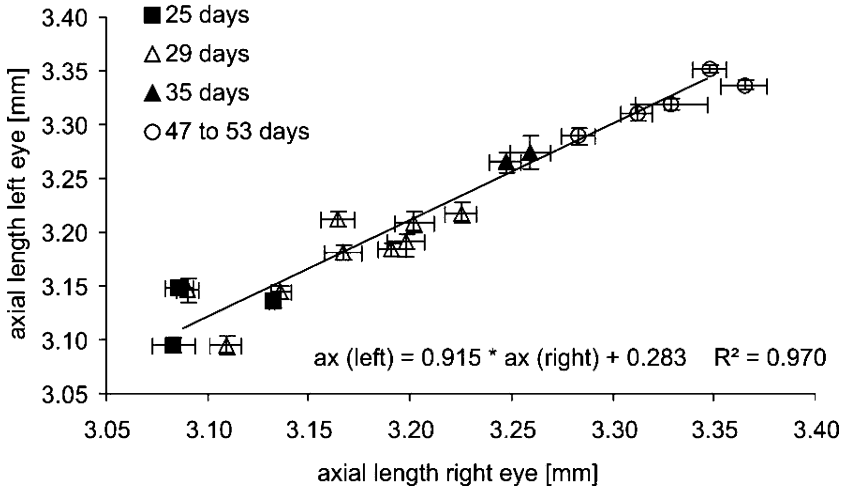

Fig. 6. Axial lengths (ax) of left and right eyes of 19 C57BL/6 mice, plotted against each other. Each data point shows the mean value of at least three OLCI scans. Error bars denote standard deviations. The average standard deviation was only 8.0 ± 4.4 μm. The equation originates from orthogonal rather than from linear regression.

were 17 ± 18 μm and, with the algebraic signs considered, −9 ± 23 μm. The inter-ocular variability in untreated animals shows that monocular deprivation must induce axial length differences of at least 20 μm to be detectable by OLCI. This axial length difference is equivalent to a change in refraction of about 4 D (Schmucker & Schaeffel, 2004).

3.1.3. Peripheral axial length as determined by OLCI

Axial length measurements with the pupil axis of the eyes tilted relative to the measurement beam by 52 ± 6° in the nasal, temporal, superior and inferior direction show that there are small, but significant differences in the OLCI scans in the periphery in both meridians (horizontal meridian, Fig. 7A: temporal −18 ± 21 μm, $p = 0.022$; nasal −3.7 ± 11 μm, n.s.; vertical meridian, Fig. 7B: superior −14.5 ± 15.3 μm, $p = 0.01$; inferior −12.1 ± 10.6 μm, $p = 0.003$; unpaired t-tests). The average standard deviations obtained in single eyes were 8.0 ± 2.4 μm for the peripheral measurements which is not different from standard deviations obtained in the pupil axis.

It is clear, however, that variations in angular alignment of a few degrees are not a major contributing factor to measurement variability.

3.1.4. Corneal thickness measurements

A comparison of corneal thickness as measured by OLCI and from frozen sections is shown in Fig. 8A. In this case, the average standard deviations are similar with both techniques (5.0 ± 2.0 μm). Thicker corneas were measured by OLCI than in frozen sections by a factor of 1.5, which is too large to be explained by inappropriate refractive indices. The slow growth rate of corneal thickness (0.4 μm per day) was similar with both techniques. The mean absolute difference between corneal thickness in both eyes was 5.14 ± 4.83 μm (paired t-test: $p = 0.4$, not significant) and, with the algebraic sign considered, −1.35 ± 6.92 μm. The average standard deviations obtained from repeated measurements in individual eyes was 3.5 ± 2.1 μm.

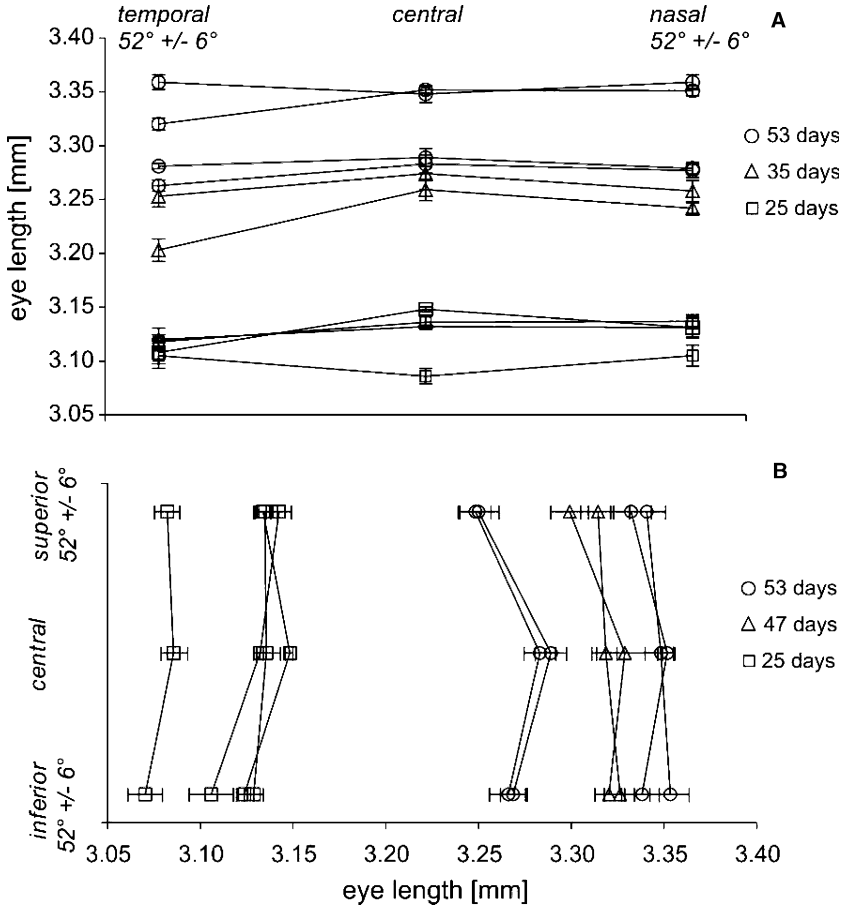

Fig. 7. Axial length measured from different angular positions in ten mouse eyes at three different age levels. Each data point represents the mean ± standard deviation of at least three OLCI scans in single animals. (A) Axial length measurements at three angular positions in the horizontal meridian and (B) axial length measurements at three angular positions in the vertical meridian.

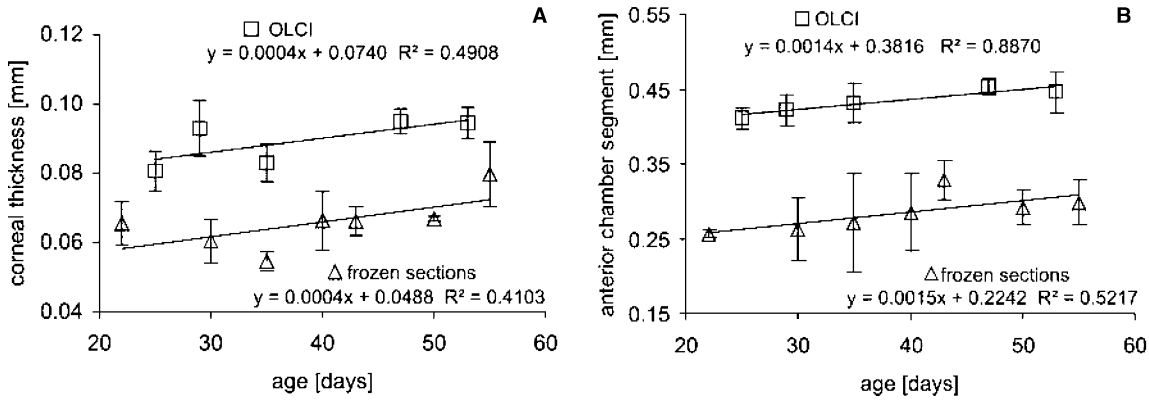

Fig. 8. Development of corneal thickness (A) and anterior chamber depth (B) in the growing mouse eye, as determined by OLCI and in frozen sections. Data from frozen sections are replotted from Schmucker and Schaeffel (2004). Error bars denote standard deviations. Note that anterior chamber depth includes corneal thickness in both data sets.

3.1.5. Anterior chamber depth

Both techniques show a similar growth rate of the anterior chamber depth (14 and 15 μm per day, respectively; Fig. 8B). Again, OLCI provides larger anterior chamber depths than frozen sections by a factor of 1.7. The average standard deviation was 20 ± 6 μm in OLCI and 35 ± 18 μm in the frozen sections (paired *t*-test; $p = 0.32$, not significant), with an average absolute difference between both eyes of 16.7 ± 14.8 μm and a difference of 5.4 ± 22 μm with the algebraic sign considered. The average standard deviation from repeated measurements in the same eyes was 10.6 ± 12.3 μm.

3.2. Effects of deprivation of form vision on refractive development and ocular growth

After two weeks of form deprivation, refraction data could be obtained from six animals. In mouse 7, the pupil was too small to obtain reliable refractions. Despite two weeks of deprivation, no significant differences were detected between the refractions of both eyes (deprived: +6.78 ± 5.19 D, control: +5.66 ± 5.27 D). Refractive development of individual animals are shown in Fig. 9A and B, respectively. In addition, both figures show the refractive development of untreated mice, replotted from Schmucker and Schaeffel (2004). In our sample, the eyes that were occluded, were more hyperopic at the begin of the experiment than the control eyes (+6.67 ± 1.61 D versus +3.54 ± 3.33 D) and this difference was almost significant (paired *t*-test; $p = 0.077$). Therefore, the change in refraction during the deprivation period relative to the start-up value was also studied. However, there was still only a tendency to develop relatively more myopia in the occluded eyes (change: +0.10 D versus +2.12 D in the open eyes) which did not achieve significance (paired *t*-test; $p = 1.67$).

Axial length data from occluded and open control eyes are shown in Fig. 10A and B. OLCI revealed axial elongation in the occluded eye, compared to the open fellow eye of 38 ± 36 μm (3.274 ± 0.027 mm versus 3.236 ± 0.039 mm; paired *t*-test; $p = 0.045$). The significance was achieved even though two animals (mouse 2 and mouse 3) responded in reversed fashion. The average absolute difference between both eyes was 47 ± 23 μm, compared to 17 ± 18 μm in untreated animals (see above). Even though the changes in eye growth were not always in the direction of more myopia, it is clear that occlusion caused more variability in axial eye growth. On average, the deprived eyes grew 1.16% more than the open fellow eyes.

It was striking that no significant myopic shift was induced by deprivation in this sample (Fig. 9), despite that there was significant axial elongation. A possible explanation could be that the dioptric apparatus decreased its refractive power. To increase the focal length, either the cornea could have flattened, the lens could have thinned or the anterior chamber depth could have deepened. On average, there was indeed a tendency of the anterior chamber depth to increase (Fig. 11A and B) in deprived eyes compared to the fellow control eyes (466 ± 29 μm versus 448 ± 21 μm). However, a paired *t*-test did not reveal significance ($p = 0.41$).

4. Discussion

A new technique is described which provides, for the first time, high resolution biometrical data of mouse eyes in vivo. Axial eye length, corneal thickness and anterior chamber depth were measured with very good repeatability and very small standard deviations (axial length: 8 μm, corneal thickness: 3.5 μm, and anterior chamber: depth 10.6 μm). OLCI achieves a significant improvement in performance over current techniques to measure small eyes (caliper measurements in excised eyes, Beuerman et al., 2003; biometry in frozen sections, Remtulla

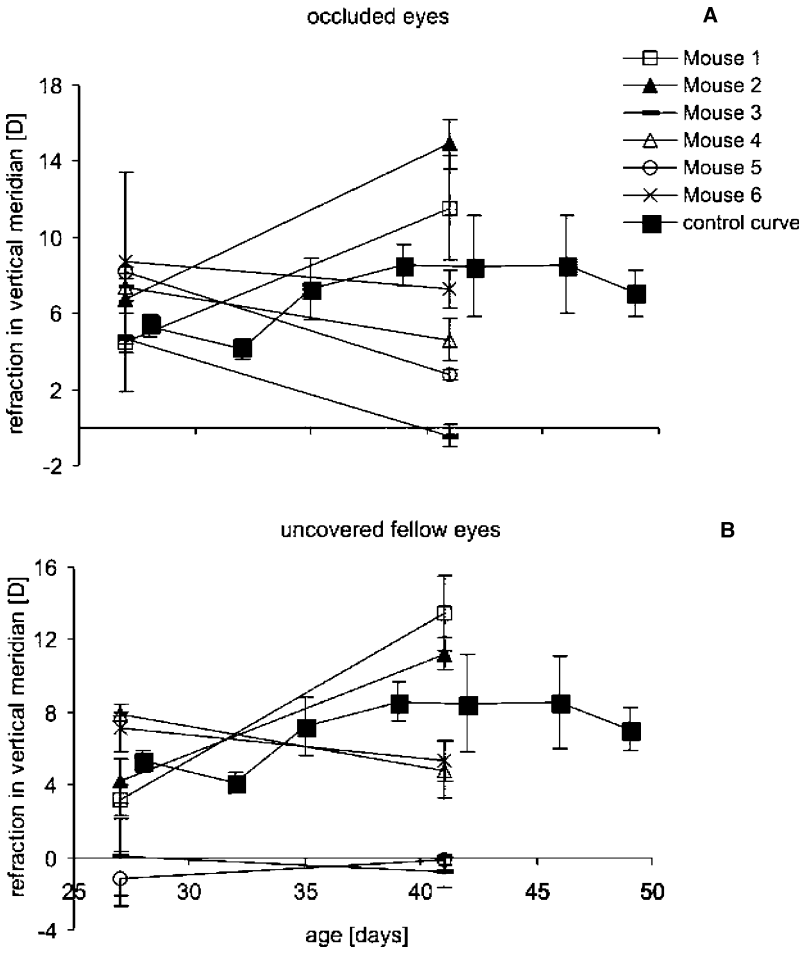

Fig. 9. Refractive development in monocularly deprived mice. Refractive error was measured by infrared photoretinoscopy at the begin of the deprivation period (day 27) and at the end (day 41). The filled squares ("control curve") show the refractive development of three untreated mice from a previous study (Schmucker and Schaeffel, 2004). (A) Refractive development in occluded eyes and (B) refractive development in open fellow eyes.

& Hallett, 1985, Schmucker & Schaeffel, 2004), or measurements in standard histological sections of fixated tissue (Tejedor & de la Villa, 2003).

4.1. Accuracy of the OLCI

4.1.1. Axial eye length measurements

Using OLCI, axial length could be determined with a mean standard deviation of 8.0 ± 2.9 μm, which is equivalent to refractive changes in mouse eyes in the range of 2 D (Schmucker & Schaeffel, 2004). Hitzenberger (1991) measured axial eye length by laser doppler interferometry using partially coherent light in emmetropic human subjects with a standard deviation of ±30 μm (about ± 0.1%). Relative to eye size, 8.0 μm is still about the resolution (about ± 0.25%) which is satisfactory given the tiny size of the mouse eye.

Biometric data of axial length from OLCI and from frozen sections were highly correlated (regression line: OLCI data=frozen section data * 1.173 − 0.354, $R^2 = 0.870$). The consistent offset of about 200 μm between both techniques is explained from the fact that frozen sections provide data on geometrical length and the OLCI technique on optical path length. To convert one into the other, the refractive indices along the optical path must be known. The major source of error must be the lens which has a much higher refractive index than the default index that is used by the software in the "ACMaster". The lens makes up approximately 60% of the total path length when the measurement beam travels through the eye (Schmucker & Schaeffel, 2004). Even though the measurement beam is aligned with optical axis of the lens, the refractive index gradient in the lens, common to all vertebrate eyes (Campbell, 1984), determines the average index along the optical path. The internal structure of the refractive index gradient is difficult to measure in detail (Acosta, Vazquez, Smith, & Garner, 2003) and it is also variable among individual eyes (Artal, Berrio, Guirao, & Piers, 2002). Therefore, the effective lens index can only be estimated

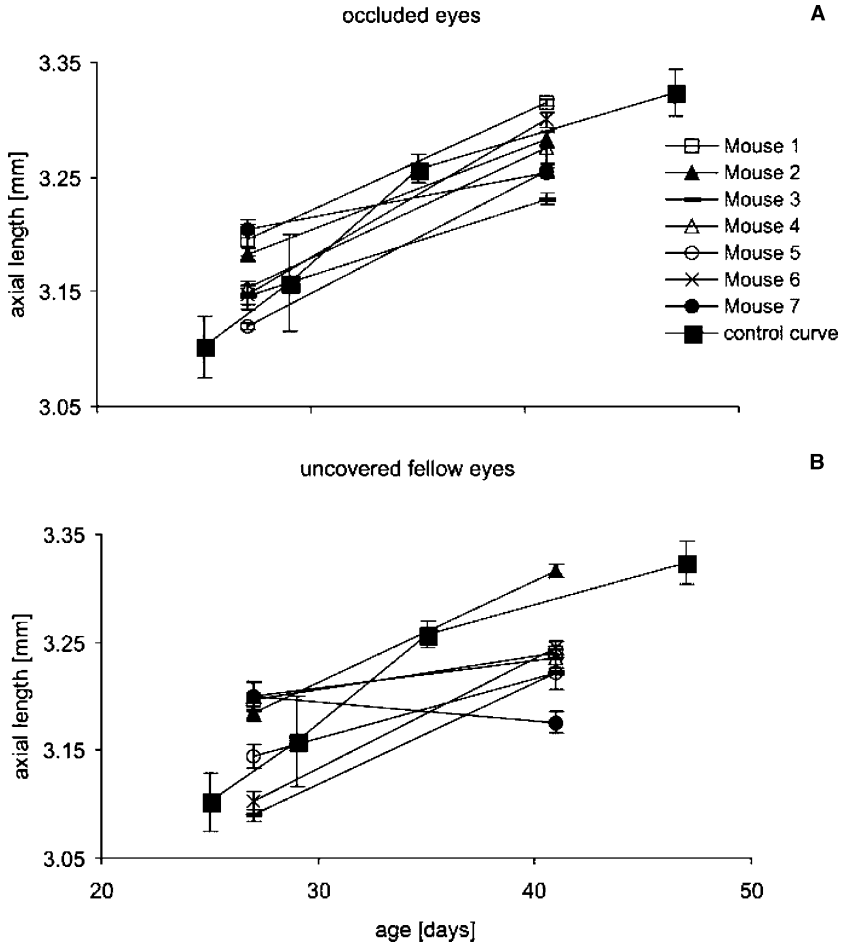

Fig. 10. Axial eye growth in the same mice described in Fig. 9. Axial eye growth data from 23 untreated control mice (from Fig. 4) are also shown for comparison. (A) Axial eye growth in occluded eyes and (B) axial eye growth in open fellow eyes.

by searching the best match of both sets of axial length data. This was achieved with an average refractive index of $n = 1.433$.

4.1.2. Corneal thickness

Recently, Schulz et al. (2003) have measured corneal thickness using optical low coherence reflectometry (OLCR) in mice in vivo. They found a mean corneal thickness of 106 ± 3.45 μm in eight 4-month-old male mice of the balb-c inbred strain. Jester et al. (2001) measured corneal thickness in adult transgenic mice using contact in vivo confocal microscopy and found a corneal thickness of 112.9 ± 7.0 μm in eight non-treated PEPCK-TGFß over-expressing mice. Schmucker and Schaeffel (2004) determined corneal thickness in the growing C57BL/6 mouse and found a linear growth rate between 22 and 100 days of age (corneal thickness=0.0003 * age + 0.0551, $R^2 = 0.45$), predicting a corneal thickness of 91 μm at 4 months of age. The data from the OLCI technique in this paper (Fig. 8A) predict a corneal thickness of 122 μm at the age of 4 month. Schulz et al. (2003) reported that corneal thickness could be measured with a standard deviation of 3.45 μm. They also found that it did not differ significantly in the right and left eye (mean difference: -0.84 ± 4.57 μm). This is similar to our findings (mean SD: 3.5 μm; mean difference between right and left eye: -1.35 ± 6.92 μm).

4.1.3. Anterior chamber depth

The average standard deviation of anterior chamber depth measurements was 10.6 ± 12.3 μm. Drexler et al. (1997) measured the anterior chamber depth in the human eye by partial coherence interferometry and found a standard deviation of 8.7 μm (range: 3.9–16.8 μm) for non-cyclopleged eyes and 1.9 μm (range: 1.7–2 μm) for cyclopleged eyes. These results showed that the variability of OLCI in human eyes can be reduced by a factor of 5 when cycloplegia is performed. However, since there is no convincing evidence for accommodation in mice (Artal, Herreros de Tejada, Munoz Tedo, & Green, 1998), is it unlikely that cycloplegia would have reduced the variability in the present study.

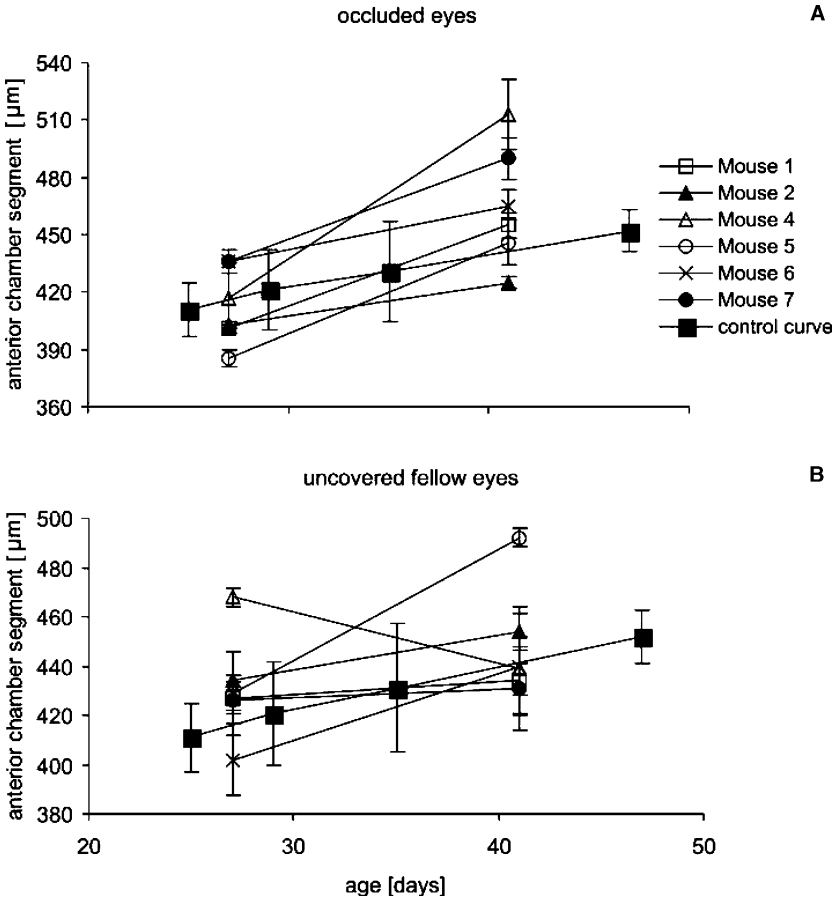

Fig. 11. Development of anterior chamber depth in the monocularly deprived eyes described in Fig. 10. In mouse 3, no anterior chamber depth data were obtained, as the anterior lens surface was not detected by the OLCI. Data on the development of the anterior chamber depth in 23 untreated mice is shown for comparison. (A) Anterior chamber depth in occluded eyes and (B) anterior chamber depth in the open fellow eyes.

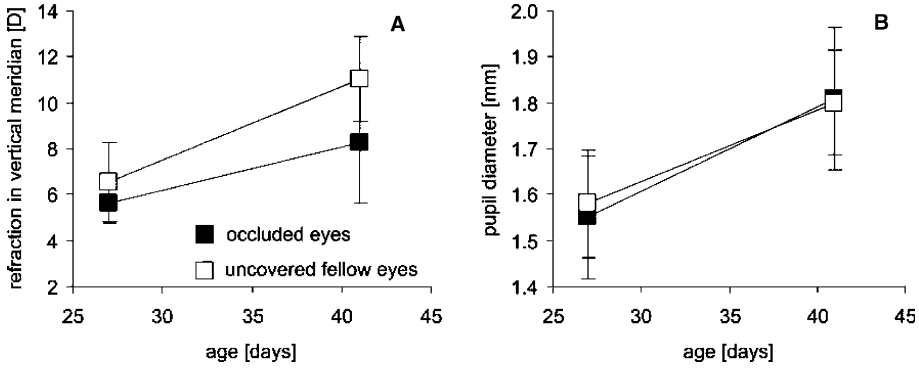

Fig. 12. A. Average refractive development in 50 mouse eyes that were covered by diffusers from day 27 to 41 (filled squares), compared to the refractive development in their open fellow eyes (open squares). Note that the average difference in refractions after 2 weeks is small (2.77 ± 3.33 D) but is still highly significant in a paired t-test ($p < 0.0001$). B. Since pupil size may be a confounding variable in measurements of refractive state (Schaeffel et al., 2004), it was verified that the pupil sizes did not differ in both eyes. The averages include previously published (Schaeffel et al., 2004), and new data.

4.2. Myopia and axial elongation during deprivation of form vision

In the current sample, no significant deprivation myopia could be detected after 14 days of deprivation. It was previously observed that mice do not always develop myopia in response to deprivation (Fernandes et al., 2004; Schaeffel et al., 2004). An extended analysis of data from 50 mice that were studied earlier and for which no OLCI data are available, shows that the

myopic shift in occluded eyes is highly significant but variable and not very large (Fig. 12).

Therefore, the lack of a significant myopic shift in the seven mice studied with the OLCI is not so unexpected. The lack of a significant shift in the myopic direction in the current sample could be explained if there were other biometric changes in the eyes that counter-balanced the effects of axial elongation. There was, on average, an increase in anterior chamber depth of 17.33 ± 43.16 μm in the deprived eyes. Simple ray tracing predicts that the shift in lens position would produce more hyperopia of about 1.7 D. Although this cannot fully counterbalance the shift in myopic direction expected from axial elongation, it is into the right direction.

5. Summary

It was demonstrated that Optical Low Coherence Interferometry (OLCI) is a powerful technique to resolve tiny differences in ocular biometry in living mouse eyes. Its resolution is sufficient to detect axial length changes of 8 μm, equivalent to only 2 D. However, the natural variability of the interocular differences between both eyes (about 18 μm) requires that changes are induced by deprivation in the range of 20 μm, equivalent to 4 D, to be reliably detected.

Acknowledgment

The authors thank R. Bergner and R. Barth from Carl Zeiss Meditec AG, Jena, Germany, for making the "ACMaster" available and for invaluable instructions on its usage.

References

Acosta, E., Vazquez, D., Smith, G., & Garner, L. (2003). A comparison and analysis of various techniques for determining the gradient index distribution of non-symmetric crystalline lenses. Available from: http://research.opt.indiana.edu/Meetings/Mopane2003/Acosta/Acosta.pdf.

Artal, P., Berrio, E., Guirao, A., & Piers, P. (2002). Contribution of the cornea and internal surfaces to the change of ocular aberrations with age. *Journal of the Optical Society of America A, Optics, Image Science, and Vision, 19*, 137–143.

Artal, P., Herreros de Tejada, P., Munoz Tedo, C., & Green, D. G. (1998). Retinal image quality in the rodent eye. *Visual Neuroscience, 15*, 597–605.

Beuerman, R. W., Barathi, A., Weon, S. R., & Tan, D. (2003). Two models of experimental myopia in the mouse. *Investigative Ophthalmology and Visual Science, 44*(Suppl.), 4338.

Campbell, M. C. W. (1984). Measurement of refractive index in an intact crystalline lens. *Vision Research, 24*, 409–415.

Drexler, W., Baumgartner, A., Findl, O., Hitzenberger, C. K., Sattman, H., & Fercher, A. F. (1997). Submicrometer precision biometry of the anterior segment of the human eye. *Investigative Ophthalmology and Visual Science, 38*, 1304–1313.

Fernandes, A., Yin, H., Byron, E., A Iuvone, P., M Schaeffel, F., Williams, R. W., & Pardue, M. T. (2004). Effects of form deprivation on eye size and refraction in C57BL/6J mice. *Investigative Ophthalmology and Visual Science* (ARVO E-Abstract, 4280/B741).

Hitzenberger, C. K. (1991). Optical measurement of the axial eye length by laser doppler interferometry. *Investigative Ophthalmology and Visual Science, 32*, 616–624.

Hung, L. F., Crawford, M. L., & Smith, E. L. (1995). Spectacle lenses alter eye growth and the refractive status of young monkeys. *Nature Medicine, 1*, 761–765.

Jester, J. V., Lee, Y. G., Li, J., Chakravarti, S., Paul, J., Petroll, W., & Cavanagh, H. D. (2001). Measurement of corneal sublayer thickness and transparency in transgenic mice with altered corneal clarity using in vivo confocal microscopy. *Vision Research, 41*, 1283–1290.

Rada, J. A., Nickla, D. L., & Troilo, D. (2000). Scleral changes associated with form deprivation myopia in mature primate eyes. *Investigative Ophthalmology and Visual Science, 41*, 2050–2058.

Remtulla, S., & Hallett, P. E. (1985). A schematic eye for the mouse and comparison with the rat. *Vision Research, 25*, 21–32.

Schaeffel, F., Bartmann, M. L., Hagel, G., & Zrenner, E. (1995). Studies on the role of the retinal dopamine/melatonin system in experimental myopia in chickens. *Vision Research, 35*, 1247–1264.

Schaeffel, F., & Burkhardt, E. (2002). Measurement of refractive state and deprivation myopia in the black wildtype mouse. *Investigative Ophthalmology and Visual Science, 43*(Suppl.), 182.

Schaeffel, F., Burkhardt, E., Howland, H. C., & Williams, R. W. (2004). Measurement of refractive state and deprivation myopia in two strains of mice. *Optometry and Vision Science, 81*, 99–110.

Schaeffel, F., & Howland, H. C. (2003). Axial length changes in myopic mouse eyes. *Investigative Ophthalmology and Visual Science, Electronic letter, 25*(April), 2003.

Schaeffel, F., Simon, P., Feldkaemper, M., Ohngemach, S., & Williams, R. W. (2003). Molecular biology of myopia. *Clinical and Experimental Optometry, 86*, 295–307.

Schmucker, C., & Schaeffel, F. (2004). A paraxial schematic eye model for the growing C57BL/6 mouse. *Vision Research, 44*, 1857–1867.

Schulz, D., Iliev, M. E., Frueh, B. E., & Goldblum, D. (2003). In vivo pachymetry in normal eyes of rats, mice and rabbits with the optical low coherence reflectometer. *Vision Research, 43*, 723–728.

Tejedor, J., & de la Villa, P. (2003). Refractive changes induced by form deprivation in the mouse eye. *Investigative Ophthalmology and Visual Science, 44*, 32–36.

Troilo, D., Nickla, D. L., & Wildsoet, C. F. (2000). Form deprivation myopia in mature common marmosets (Callithrix jacchus). *Investigative Ophthalmology and Visual Science, 41*, 2043–2049.

Zhou, G., & Williams, R. W. (1999). Eye1 and Eye2: gene loci that modulate eye size, lens weight, and retinal area in the mouse. *Investigative Ophthalmology and Visual Science, 40*, 817–825.